Desalination and Water Treatment
www.deswater.com

doi: 10.5004/dwt.2022.28374

256 (2022) 242–252
April

2,2′-Dithiobis(2,3-dihydro-1,3-benzothiazole) as an effective inhibitor for carbon steel protection in acid solutions

Mahmoud G.A. Saleh[a], S. Abd El Wanees[b,c,*]

[a]*Chemistry Department, Faculty of Science, Northern Border University, Arar, Saudi Arabia, email: mgsaleh72@yahoo.com (M.G.A. Saleh)*
[b]*Chemistry Department, Faculty of Science, Zagazig University, Zagazig, Egypt, email: s_wanees@yahoo.com (S. Abd El Wanees)*
[c]*University College of Umluj, Umluj, Tabuk University, Tabuk, Saudi Arabia, email: s_nasr@ut.edu.sa (S. Abd El Wanees)*

Received 29 September 2021; Accepted 4 March 2022

ABSTRACT

2,2′-Dithiobis(2,3-dihydro-1,3-benzothiazole), DTDBT, was used to mitigate the destructive effect of 0.5 M HCl on the C-steel surface. Gravimetry, potentiodynamic polarization, and electrochemical impedance spectroscopy, techniques as well as scanning electron microscopy complemented with energy-dispersive X-ray analysis for some corroded steel samples were employed. The data of different techniques were compatible and confirmed the inhibition effect of DTDBT. The potentiodynamic polarization data disclosed that the DTDBT molecules behave as a mixed-kind inhibitor. The different thermodynamic factors for the corrosion and adsorption processes were deduced to suggest the inhibition mechanism. The DTDBT molecules are adsorbed on the C-steel surface confirming the Langmuir isotherm according to a mixed mechanism (physical and chemisorption).

Keywords: Benzothiazole; Gravimetry; Potentiodynamic polarization; Corrosion inhibitor; Impedance; Adsorption

1. Introduction

Carbon steel is mightily employed as the structural matter in various fields owing to the outstanding mechanical characteristics and relatively little price [1,2]. Acid solutions are employed in the different fields for the production processes, and the different usages, such as acid pickling, acid purifying, acid de-scaling, and oil well cleaning [3]. The advantages of using HCl over others acids are less pickling time, lower temperature as well as better surface quality. The deleterious effect of using acids oxidizes the industrial and metal containers, lowering the production and causing economic loss [4]. Due to the destructive effect of HCl solutions on metallic surfaces, inhibitors are substantial to reduce the aggressive effect on the steel surface [5]. The effective organic molecules are generally used in small quantities in acid solutions to tolerate severe corrosion [6]. The chosen of the selected materials as inhibitors depend on many factors among of these is the economic purpose and the other is the molecular structure should include an aromatic ring with an electron cloud and/or the electronegative centers like S, N, and O atoms in the relatively long-chain compounds [7]. Such of these organic molecules have been mightily utilized as efficacious retarders towards the acid destruction of steel.

Benzothiazole derivatives have been employed as suitable retarders for the destruction of steel in acidic aqueous solutions [8,9], zinc in HCl [10] and copper in NaCl solutions [11]. The molecules of benzothiazole are characterized by the existence of an aromatic ring including sulfur and nitrogen atoms, which are rich in electrons densities and display active centers for the inhibition process. The mechanism of inhibition of such compounds was found to depend on the adsorption process on the metal

* Corresponding author.

surface as well as the inhibitor concentration and temperature. The efficient adsorption could have resulted from the presence of the π-electrons inside the selected molecule beside the unsaturated bonds formed in the presence of the heteroatoms (S or O or N) in the inhibitor's molecular composition [12].

Our work aims to explore the inhibition performance of 2,2′-dithiobis(2,3-dihydro-1,3-benzothiazole), DTDBT, as an efficient retarder against the destruction of C-steel in 0.5 M HCl solutions. The material of DTDBT is an easily prepared laboratory with a high yield that is soluble in dilute acid solutions. Gravimetric, potentiodynamic polarization, and electrochemical impedance spectroscopy (EIS) were utilized. Some of the thermodynamic parameters of the corrosion and adsorption processes were calculated and explored.

2. Experimental part

2.1. Working electrode

All working coupons and electrodes for the experimental study were prepared from C1018 low carbon steel. The components of this kind of steel are clarified in Table 1. The coupons and electrodes were abraded with various series of polished papers, washed thoroughly with bi-distilled water, degreased, and dried with acetone. The surface area of each coupon was 38.70 cm^2.

2.2. Synthesis of 2,2′-dithiobis(2,3-dihydro-1,3-benzothiazole)

The used inhibitor was prepared laboratory by a transformation reaction of a thiol compound into disulfide by using an ammonium persulfate salt in the presence of ethylenediamine [13]. 2,3-Dihydro-1,3-benzothiazole-2-thiol (10 mmol) was mixed thoroughly with ethylenediamine (5 mmol). The ammonium persulfate (11 mmol) was added with a continuous mixing using pestle and mortar for a while 40 min. After the accomplishment of the reaction, the crude product was extracted by using a dichloromethane solvent. The removal of the solvent under reduced pressure and the yield was recrystallized using ethanol to give a purity of 87%. The synthetic route for the synthesis of 2,2′-dithiobis(2,3-dihydro-1,3-benzothiazole) (inhibitor) is shown in Fig. 1.

2.3. Electrochemical measurements

The electrochemical experimental are included the potentiodynamic polarization, *E-i* curves, and the EIS were executed on a Voltalab 40 Potentiostat PGZ 301. The used electrolytic cell was formerly described [14], which is provided with many electrodes as a Pt foil, a saturated calomel, and C-steel (SCE) as an auxiliary, a reference, and a working electrode (WE), respectively. A small cylindrical rod of low C-steel (WE) was settled to a borosilicate glass tube with an Araldite leaving the cross-sectional surface area of 0.28 cm^2. The C-steel electrodes were polished with a series of various polished papers and washed using distilled water and acetone. The WE was immersed in the investigated solution under the open circuit situation for 60 min until a steady-state potential, E_{st} was attained. The polarization data were gained by sweeping the WE potential between –800 and –200 mV, at E_{corr} with a sweeping rate of 1 mV/s, at 298 K. To ensure the repeatability of the results, each experiment was duplicated and the data were identical.

The impedance spectra curves were obtained when a small alternating voltage perturbation (10 mV) was utilized on the electrolytic cell. The range of frequency was varied between 100 kHz to 50 mHz and the EIS curves were fitted utilizing the ZSimpWin program.

2.4. Gravimetric measurements

The cleaned and dried C-steel specimens were weighed prior and next inundation in an open bottle containing a fixed amount (250 ml) of 0.5 M HCl solutions devoid of containing the DTDBT inhibitor. Trails were done at various temperatures, 298–313 K. The temperature was monitored by using a water bath equipped with thermostat control, ±1°C. The C-steel specimen was removed after 6 h, washed with distilled water two times followed by degreasing with acetone, dried, and accurately weighed. For good reproducibility, the trials were done in triplicate.

Table 1
Chemical composition (wt.%) of the C-steel

Element	Composition (wt.%)
C	0.12
Mn	0.5
Si	0.17
S	0.6
P	0.046
Fe	Rest

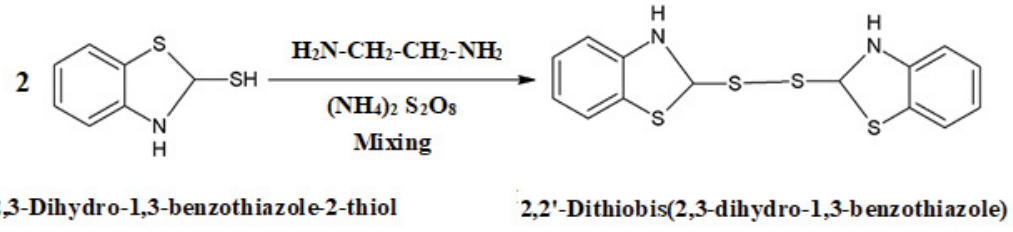

Fig. 1. Synthetic route of 2,2′-dithiobis(2,3-dihydro-1,3-benzothiazole), DTDBT.

2.5. Scanning electron microscopy and energy-dispersive X-ray investigations

The scanning electron microscopy (SEM), and energy dispersive X-ray analysis energy-dispersive X-ray (EDX) are utilized to investigate the changes in the surface morphology of some selected C-steel specimens after inundation in the examined solutions. The elemental composition of the surface film of the investigated steel samples was investigated by the EDX analysis. The working specimens were examined employing a JEOL TM Scanning Microscope JSM-T100 (Japan).

3. Results and discussion

3.1. Potentiodynamic polarization

The potentiodynamic polarization data of C-steel immersed in 0.5 M HCl solutions devoid of and containing various amounts of DTDBT inhibitor are plotted in Fig. 2. The corrosion current density (i_{corr}) has been deduced from the anodic–cathodic polarized curves by the Tafel extrapolation method. The different polarization factors like E_{corr}, i_{corr}, the cathodic (β_c), and the anodic (β_a) Tafel slopes, the protection efficacy, η_p and standard deviation, σ were determined as offered in Table 2. It is noted that the values of β_c and β_a do not display a noticeable mutation that reveals that the mechanism of the steel destruction does not alter, when the DTDBT inhibitor is added, for each of the anodic and the cathodic reactions. Also, Fig. 2 depicts that the existence of the DTDBT inhibitor displaces the anodic–cathodic polarized curves to the less active directions to give lower values of i_{corr}, which manifests that DTDBT molecules behave as a mixed-kind inhibitor [15–18].

In other words, it can be monitored that the entity of the DTDBT molecules does not have a noticeable effect on E_{corr} concerning the blank. This proves that DTDBT inhibits each of the anodic and cathodic reactions. If the displacement in the E_{corr} exceeds + 85 mV concerning the blank value will confirm that, the inhibitor is classified as either an anodic or a cathodic inhibitor [17]. However, in our study, the maximum displacement in E_{corr} was found to be within –10 to –36 mV, therefore, the DTDBT could be categorized as a mixed-kind inhibitor [15–17]. Ajmal et al. [8] indicated that 2-hydrazino-6-methyl-benzothiazole acts as an effective cathodic inhibitor for the corrosion of mild steel in HCl and mixed inhibitor in H_2SO_4 [8].

The surface coverage, θ, and the protection efficacy, η_p, of the DTDBT molecules were determined from the values of i_{corr} using the following relations [18–20]:

$$\theta = \left(1 - \frac{i_{corr}}{i^{\circ}_{corr}}\right) \quad (1)$$

$$\eta_p = 100\theta \quad (2)$$

where i°_{corr} and i_{corr} are the corrosion current density gained with the free acid and the added DTDBT molecules, successively.

The obtained data indicated that, by increasing the amount of the DTDBT, the protection efficacy is raised due to the reduction in the i_{corr} value. This would confirm the adsorption of the DTDBT molecules through the anodic and cathodic active centers on the C-steel surface. The rise in inhibition efficacy with inhibitor concentration explores that the DTDBT inhibitor has a good adsorptive properties towards the metal surface.

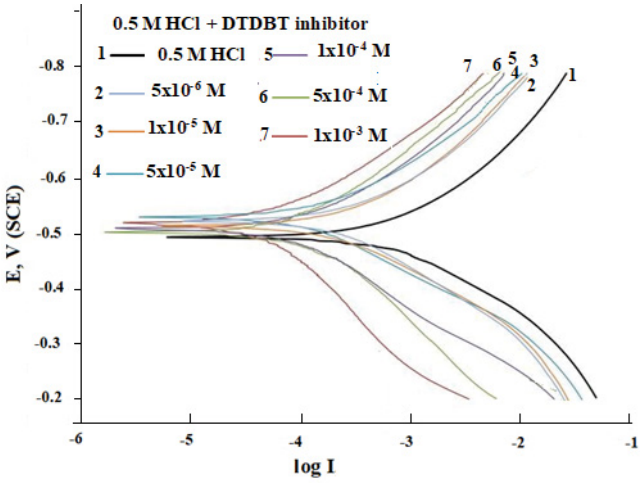

Fig. 2. Potentiodynamic polarization curves of C-steel in 0.5 M HCl solution without and with different additions of DTDBT inhibitor.

Table 2
The corrosion parameters, E_{corr}, i_{corr}, cathodic Tafel slope (β_c), anodic Tafel slope (β_a), protection efficacy, η_p and standard deviation, σ for C-steel immersed in 0.5 M HCl containing different concentrations of DTDBT inhibitor, at 298 K

Conc., M	$-E_{corr}$, mV	β_a, mV/dec	$-\beta_c$, mV/dec	i_{corr}, mA/cm²	θ	η_p %	σ
Free acid	501	289	199	1.04	–	–	
5×10^{-6}	531	182	200	0.58	0.44	44.1	0.69
1×10^{-5}	522	150	192	0.44	0.58	57.5	1.27
5×10^{-5}	539	128	149	0.23	0.78	78.1	1.22
1×10^{-4}	517	188	161	0.16	0.85	84.6	0.20
5×10^{-4}	511	137	151	0.09	0.91	90.9	0.75
1×10^{-3}	527	250	142	0.069	0.93	93.4	0.86

The standard deviation values, σ, of the protection efficacy listed in Table 2 are varied between 0.2 and 1.27 depending on the DTDBT concentration that manifests the good agreement between the different techniques. It is noteworthy to find that the DTDBT inhibitor is similar in the inhibition ability with some other benzothiazoles compounds [8,9]. The high values of the inhibition efficiency of the DTDBT molecules could be attributed to the increase in the adsorbability of such molecules. This behavior could be related to the presence of different types of heteroatoms which are rich by the lone pair of free electrons besides the presence of two aromatic rings (π-electrons on the conjugated system) which are considered as active centers for adsorption on the metallic surface to form a protective layer.

3.2. EIS investigations

The Nyquist plots of C-steel in 0.5 M HCl solution without and with various additions of DTDBT molecules are represented in Fig. 3. The obtained impedance data have considerably changed with the existence of DTDBT molecules. The gained impedance spectra data can be explicated within the equivalent circuit of the electric double layer (Fig. 4) that has been utilized formerly for the Fe-acid interface [21].

As can be indicated in Fig. 3, the impedance spectra offer an individual capacitive loop as performed by a little dejected semi-circle in the presence of the used inhibitor, not exemplary semicircles as expected from EIS theory for assumed equivalent circuit. The presence of the capacitive loop confirms that the charge transfer process dominates the destruction of metal with the existence of a preventative layer on the C-steel when the DTDBT molecules are added [22]. The depression in the Nyquist plot of the semicircles spectra of Fig. 3 is generally pointed to the heterogeneity of the metal surface owing to the grossness of the metal surface or interfacial phenomena [23,24]. The diameter of the capacitive loops is elongated gradually with raising the added amount of the DTDBT molecules, indicating a strengthening of the formed inhibitive film.

The symmetric Bode and phase angle curves acquired for the C-steel surface in 0.5 M HCl in the absence and presence of the various amounts of DTDBT inhibitor are shown in Fig. 5. It is clear that, at the low-frequency zone, the values |Z| are raised, which would establish the rise in the inhibition efficacy with higher additions of the used inhibitor. This could be related to the adsorption of the DTDBT molecules through the lone pair of electrons of the active centers on the C-steel surface protecting it from the acid attack [25]. In addition to this, the displacement of the phase angle into the more negative values confirms the presence of an insulating film protecting the surface of the C-steel from the corrosion process [25,26].

The electrochemical impedance parameters such as the charge transfer resistance, R_{ct}, double layer capacitance, C_{dl}, and the percent of protection efficacy, η_I, are calculated from the analysis of Nyquist plots, Table 3. The protection efficacy (η_I) was determined according to Eq. (3) [27,28]:

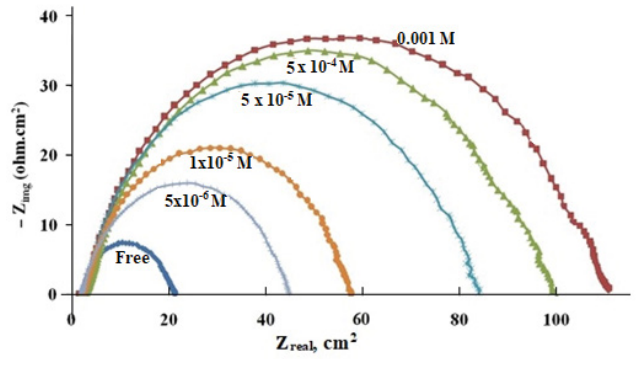

Fig. 3. Nyquist plots of C-steel in 0.5 M HCl solution without and with different additions of DTDBT inhibitor.

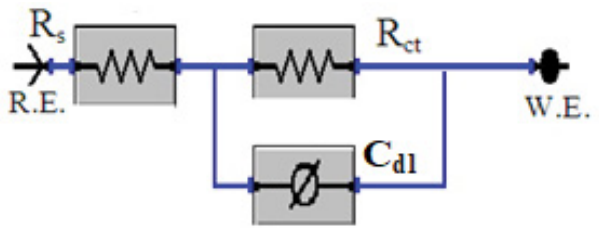

Fig. 4. Equivalent circuit model is used to fit the EIS data in the absence and presence of DTDBT inhibitor.

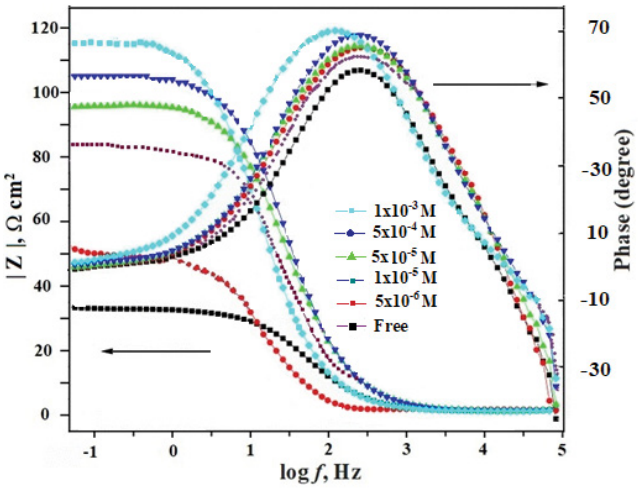

Fig. 5. Bode and phase angle plots of C-steel in 0.5 M HCl devoid of and containing different amounts of DTDBT inhibitor.

Table 3
EIS data for corrosion of C-steel in 0.5 M HCl devoid of and containing different amounts of DTDBT inhibitor, at 298 K

Conc., M	C_{dl}, μF/cm²	R_{ct}, Ω cm²	θ	η_I
Blank	124.3	20.22	–	–
5×10^{-6}	103.7	42.95	0.425	42.48
1×10^{-5}	72.48	54.89	0.545	54.53
5×10^{-5}	55.08	80.89	0.806	80.64
5×10^{-4}	35.20	90.40	0.902	90.18
1×10^{-3}	37.26	95.65	0.954	95.44

$$\eta_I\% = \left(\frac{R_{ct} - R^{\circ}_{ct}}{R_{ct}} \right) \quad (3)$$

where R°_{ct} and R_{ct} are the charge transfer resistance in the case of the free acid and in the presence of the DTDBT molecules, successively. The different values of the C_{dl} were deduced from the relation [29]:

$$C_{dl} = Y_o \left(\omega_{max} \right)^{n-1} \quad (4)$$

where $\omega_{max} = 2\pi f_{max}$ and f_{max} is the frequency at which the imaginary component of the impedance is the topmost.

The increases in R_{ct} values with the additions of the DTDBT molecules could be suggested the adsorption of the inhibitors molecules on the metallic surface [25]. On the other hand, the reduction in the C_{dl} values when the DTDBT molecules are added could be attributed to the rise in the density of the electrical double layer confirming the reduction in the corrosion rate due to the adsorption process [25,26].

3.3. Mass loss investigations

The loss in weight mensuration is employed to confirm the inhibition achievement of C-steel corrosion in 0.5 M HCl without and with the additions of different amounts of DTDBT molecules. The data of weight loss are used to determine various corrosion factors such as corrosion rate (r_{corr}, μg/cm²/h), θ, and the protection efficacy (η_w), Table 4. The value of r_{corr} was deduced utilizing the equation [30]:

$$r_{corr} = \frac{\left(W - W' \right)}{At} \quad (5)$$

where W and W' are the weight losses of C-steel coupons before and after immersion in the investigated solution, A is the contact surface area of the C-steel, and t is the immersion time.

The values of θ and the protection efficacy (η_w) of the DTDBT inhibitor was determined, respectively, from the relations [31]:

$$\theta = \left(1 - \frac{r_{corr}}{r_{corr.inh}} \right) \quad (6)$$

$$\eta_w = \theta\left(100\right) \quad (7)$$

where r_{corr} and $r_{corr\text{-}inh}$ are the weight loss values in the case of 0.5 M HCl without and with the added DTDBT molecules, respectively. The data indicates that the r_{corr} is reduced as the amount of DTDBT is increased and is raised with the temperature with the free acid and the inhibited solutions. The presence of higher additions of DTDBT inhibitor decreases the r_{corr} and raises the inhibition efficiency values, η_w, Table 4. The sigmoid nature of η_w – logC_{inh} curves, of Fig. 6 could confirm the adsorptive ability of the DTDBT inhibitor towards the metal surface [31]. The reduction in the protection efficacy values, η_w, with the inhibitor concentrations, at high temperatures (Fig. 6) could be related to the desorption of some of the DTDBT molecules with the rise in the temperature [32].

3.4. Thermodynamics of adsorption process

Generally, the premier process in the toleration of the metal destruction is the adsorption of the inhibitor through the active sites on the metallic surface at the metal/solution interface forming a preventative layer that reduces the direct contact between the aqueous phase and the investigated metal. The adsorption process is found to rely on variable factors among which are the electrochemical potential of the investigated metal surface, the chemical composition of the inhibitor, and the temperature. The molecules of H_2O could easily adsorb at the metal/solution interface. So, the process of adsorption of the used inhibitor can be considered as a quasi-substitution process between adsorbed water molecules, $H_2O_{(ads)}$, and the added organic inhibitor in the aqueous phase, $DTDBT_{(sol)}$, according to [33]:

$$DTDBT_{(sol)} + x\,H_2O_{(ads)} \leftrightarrow DTDBT_{(ads)} + x\,H_2O_{(sol)} \quad (8)$$

where x refers to the number of water molecules, $H_2O_{(sol)}$, substituted by an inhibitor molecule, $DTDBT_{(ads)}$.

Table 4
Gravimetric data for corrosion of C-steel in 0.5 M HCl and in the absence and presence of different concentrations of DTDBT inhibitor, at 298 and 313 K

Conc., M	298 K			313 K		
	r_{corr}, μg/cm² min	θ	η_w %	r_{corr}, μg/cm² min	θ	η_w %
Free acid	5.720	–	–	7.530		
1×10^{-6}	3.720	0.35	35.00	6.100	0.19	19.00
5×10^{-6}	3.260	0.43	43.00	5.800	0.23	23.00
1×10^{-5}	2.574	0.55	55.00	5.570	0.26	26.00
5×10^{-5}	1.260	0.78	78.00	4.740	0.37	37.00
1×10^{-4}	0.858	0.85	85.00	3.990	0.47	47.00
5×10^{-4}	0.458	0.92	92.00	2.11	0.72	72.00
1×10^{-3}	0.343	0.94	94.00	1.656	0.78	78.00

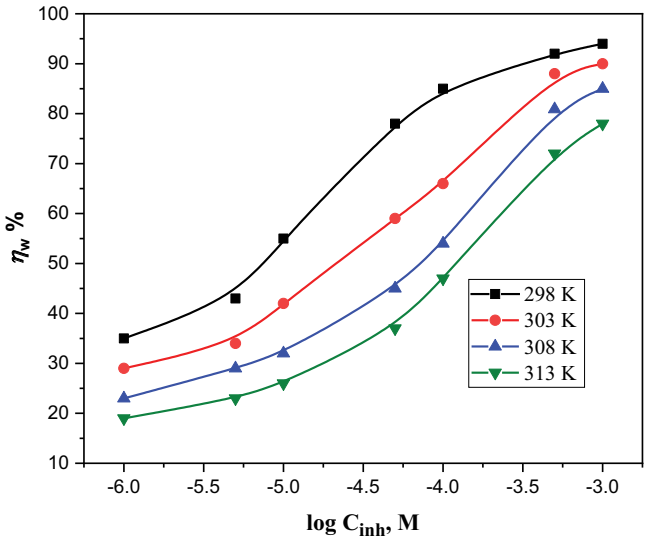

Fig. 6. Variation of the inhibition efficacy (η_w %) with logC_{inh} of DTDBT inhibitor (data obtained by gravimetric method).

The surface coverage, θ, associated with the inhibitor concentration, *C*, are employed to fit the preferable applicable adsorption model. Attempts are done to fit the different kinds of known adsorption isotherms. The more suitable type was Langmuir, which has a simple representative form [34]:

$$\frac{C}{\theta} = \frac{1}{K_{ads}} + C \tag{9}$$

As elucidated in Fig. 7, the relation between $C\theta^{-1}$ and *C* introduced a straight-line relation, with a slope around unity, confirming the adsorption of the DTDBT molecules in 0.5 M HCl obeying the Langmuir model. The intercept of the straight-line $C\theta^{-1}$ axis was equal to the inverse of the adsorption equilibrium constant $(K_{ads})^{-1}$. The high value of K_{ads} confirms the high adsorption capacity of the DTDBT molecules on the metal surface. The decrease in K_{ads} value with temperature (Table 5) could be related to the reduction in the adsorption ability of the added DTDBT molecules on the metal surface confirming the decrease in the inhibition achievement [35].

The standard free energy of adsorption, ΔG°_{ads}, can be deduced from the relation [36,37]:

$$\Delta G^\circ_{ads} = -RT\ln\left(55.5K_{ads}\right) \tag{10}$$

where 55.5 value represents the concentration of water. According to the literature, ΔG°_{ads} values about −20 kJ/mol or higher confirm the physisorption among the used inhibitor molecules and the corroded metal surface. Furthermore, ΔG°_{ads} values about −40 kJ/mol or lower assert covalent chemical bonds formation owing to electrons sharing between the inhibitor molecules and the metal surface (chemisorption) [8]. In our results, the ΔG°_{ads} values lye between –36.51 and –34.86 kJ/mol depending on the temperature confirm that the physisorption and chemisorption mechanisms [35]. The negative values of

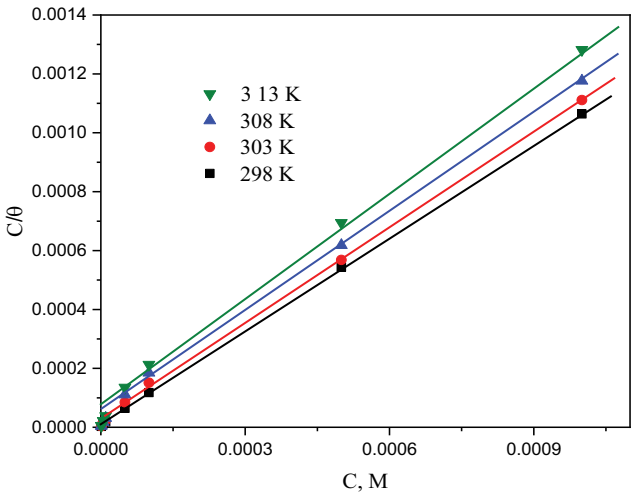

Fig. 7. Langmuir adsorption isotherm of DTDBT inhibitor on the C-steel surface in 0.5 M HCl at different temperatures.

ΔG°_{ads} explore the spontaneous adsorption of the DTDBT inhibitor through the active sites on the metal surface forming a stable adsorbed film [38,39]. Also, the decrease in ΔG°_{ads} values with temperature confirms that the protection of C-steel by the adsorbed film of the DTDBT molecules is an endothermic process [40].

The standard enthalpy, ΔH°_{ads}, can be obtained by using the Van't Hoff equation [41]:

$$\ln K_{ads} = -\left(\frac{\Delta H^\circ_{ads}}{RT}\right) + \text{constant} \tag{11}$$

The relation between the K_{ads} values and $1/T$ can be plotted, Fig. 8. A straight-line relation is gained with a slope = $-\Delta H^\circ_{ads}/R$. The negative value of the standard enthalpy, ΔH°_{ads}, Table 5, proves that the adsorption of the DTDBT molecules on the metal surface is an exothermic process [41]. This conclusion illustrates the reduction in the protection efficacy with the rise of the solution temperature, (as shown in Fig. 6). This is considered as an indication of the desorption of some of the adsorbed DTDBT molecules from the metal surface by the rise in the solution temperature. In an exothermic process, physical adsorption is featured from chemical adsorption by the gained value of ΔH°_{ads}. The obtained ΔH°_{ads} value was –71.16 kJ/mol which confirms the adsorption of the DTDBT molecules by electrostatic interaction between the charged DTDBT molecules and the charged C-steel surface [39]. In the case of the chemisorption process, ΔH°_{ads} value reaches 100 kJ/mol; while those for the physical adsorption process are less than 40 kJ/mol [42]. The calculated ΔH°_{ads} are more than that of the physical adsorption enthalpy and lower than that of the chemisorption confirming the mixed chemisorption and physisorption processes [42,43].

The standard entropy, ΔS°_{ads}, can be determined by the equation [44]:

$$\Delta G^\circ_{ads} = \Delta H^\circ_{ads} = T\Delta S^\circ_{ads} \tag{12}$$

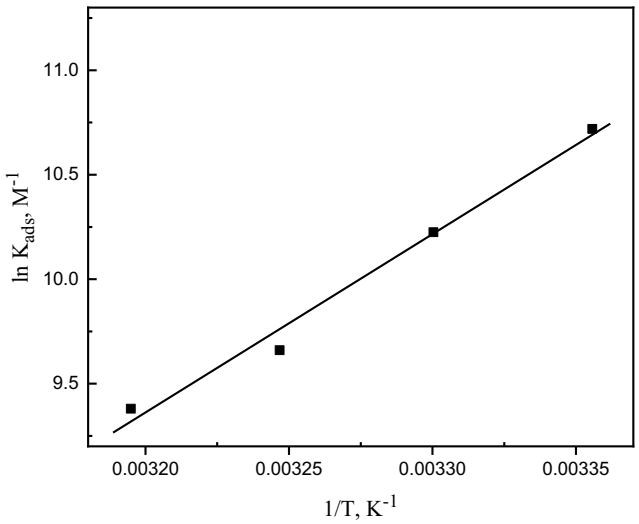

Fig. 8. Van't Hoff plots (lnK_{ads} vs. 1/T) for the adsorption of DTDBT inhibitor on the C-steel surface in 0.5 M HCl.

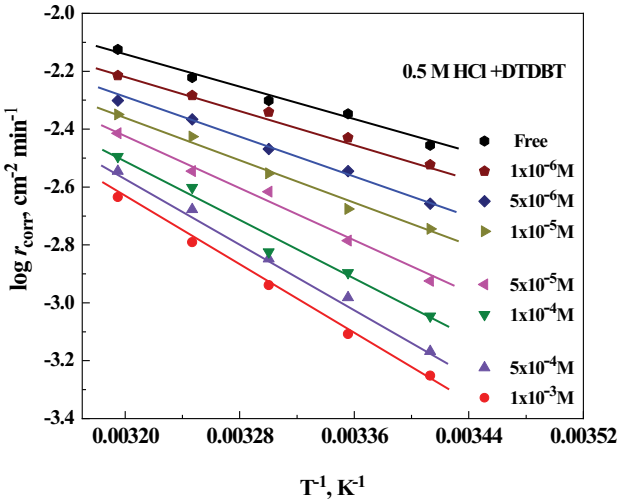

Fig. 9. Arrhenius plots (logr_{corr} vs. 1/T) for C-steel corrosion in 0.5 M HCl without and with different additions of DTDBT inhibitor.

Table 5
Thermodynamic adsorption parameters of DTDBT inhibitor on C-steel surface in 0.5 M HCl, at different temperatures

T, K	K_{ads}, M^{-1}	ΔG°_{ads}, kJ/mol	ΔH°_{ads}, kJ/mol	ΔS°_{ads}, J/mol K
298	45,223	–36.51	–71.16	–116.3
303	27,606	–35.88		–116.4
308	15,635	–35.00		–117.4
313	11,862	–34.86		–116.0

The estimated ΔS°_{ads} at different temperatures are tabulated in Table 5. The negative sign of ΔS°_{ads} could be attributed to the advancement of the adsorption process just the transfer of the DTDBT inhibitor into the metal surface. Before the adsorption process, the inhibitor molecules might diffuse freely in the bulk of the corrosive solution (the inhibitor molecules were disordered), but with the advance in the adsorption process, inhibitor molecules were systematically adsorbed on the metal surface with a reduction in the entropy of the system [13].

The negative values of ΔS°_{ads}, alludes to the higher adsorption ability of the DTDBT molecules on the metal, as attributed to the advancement of the adsorption as the DTDBT inhibitor molecules reached the C-steel surface [39,44].

3.5. Activation parameters

The rate of corrosion, W', calculated from the gravimetric data at various temperatures, Table 4, are utilized to calculate the apparent activation energy, E_a. Depending on the Arrhenius equation the values of logW' can be plotted against 1/T for the inhibited and uninhibited solutions, Fig. 9 [45].

$$\log r_{corr} = \left(\frac{-E_a}{2.303RT}\right) + \log A \quad (13)$$

where E_a refers to the apparent activation energy while A represents the pre-exponential constant. Linear relations are obtained with regression coefficients (R^2) very near to one. The deduced E_a values (obtained from, slope = $-E_a/2.303RT$) are tabulated in Table 6. The higher values of E_a gained in the case of DTDBT inhibitor with an attendant decrease in inhibition efficacy at higher temperature suggests the physisorption mechanism of the DTDBT inhibitor on the metal surface [44–48].

The transition state equation can be utilized to deduce the activation enthalpy (ΔH°) and entropy (ΔS°) [49]:

$$\log \frac{r_{corr}}{T} = \log\left(\frac{R}{Nh}\right) + \left(\frac{\Delta S^{\circ}}{2.303R}\right) - \left(\frac{\Delta H^{\circ}}{2.303RT}\right) \quad (14)$$

where R is the universal gas constant, while h and N represent the Planck's constant and Avogadro's number, respectively. The values of log (r_{corr}/T) are plotted against 1/T for C-steel in 0.5 M HCl without and with the additions of DTDBT inhibitor, Fig. 10. Straight lines with a slope equal to $-\Delta H^{\bullet}/2.303R$ and the intercept equivalent to {log(R/Nh) + $\Delta S^{\bullet}/2.303R$} are obtained. The deduced $\Delta H^{\bullet}$ and $\Delta S^{\bullet}$ values for the free acid and the various amounts of the DTDBT are tabulated in Table 6. The positive values of $\Delta H^{\bullet}$ confirm the endothermic nature of the transition state (activated complex) that reflect the difficulty of this process [37,44]. The values of the activation adsorption entropy, $\Delta S^{\bullet}$ are varied between –212 and –130 J/mol/K for all the investigated solutions. The negative values of ΔS^{*} reflect that the activated complex in the transition state process represents a combination rather than a secession process [37,44,50,51].

3.6. Surface investigation

3.6.1. SEM study

The SEM investigation is employed to explore the surface morphology of C-steel coupons before and

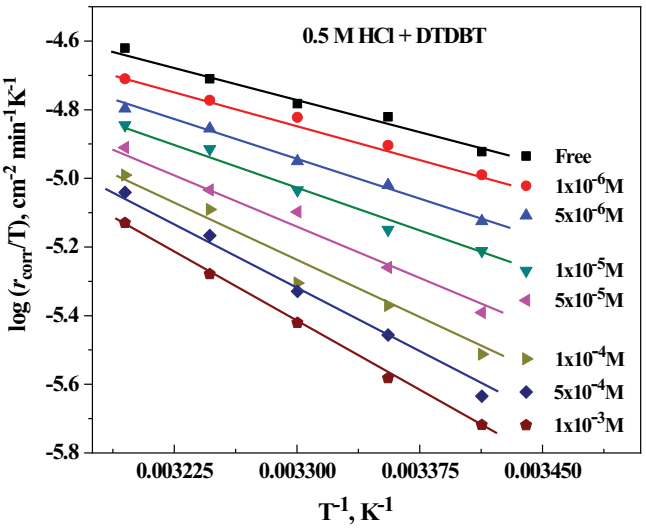

Fig. 10. Transition state plots of $\log(r_{corr}/T)$ vs. $1/T$ for the corrosion of C-steel in 0.5 M HCl without and with different additions of DTDBT inhibitor.

Table 6
Thermodynamic corrosion parameters for C-steel in 0.5 M HCl, in the absence and presence of concentrations of DTDBT inhibitor

Conc., M	E_a, kJ/mol	ΔH_a, kJ/mol	$-\Delta S_a$, J/mol
Free	26.54	23.38	212
1×10^{-6} M	26.81	24.28	210
5×10^{-6} M	32.84	28.83	198
1×10^{-5} M	36.49	36.97	172
5×10^{-5} M	42.28	41.78	158
1×10^{-4} M	49.17	46.45	145
5×10^{-4} M	54.43	51.90	128
1×10^{-3} M	56.04	51.97	130

after immersion in 0.5 M HCl for a period of 3 h solution in the absence and presence of 1×10^{-4} M DTDBT inhibitor. The SEM image of the abraded C-steel coupon before immersion in 0.5 M HCl solution, Fig. 11A, appears with a soft abraded surface with little scratches owing to the polishing process. The SEM micrograph of the polished C-steel specimen after immersion in 0.5 M HCl is depicted in Fig. 11B. This micrograph indicates a sorely damaged surface with conspicuous large pits surrounded by some of the formed corrosion products. In contrast, the micrograph of Fig. 11C represents the SEM of C-steel electrode surface after immersion in 0.5 M HCl containing 1×10^{-4} M DTDBT inhibitor. A less deteriorated cracked area on the layer formed on the C-steel surface, which means that a preventative layer has been formed on the surface of the C-steel specimen, confirming that the DTDBT behaves as an active retarder towards the corrosion of C-steel in 0.50 M HCl.

3.6.2. EDX study

The EDX investigation was carried out in order to identify the element composition on the surface of C-steel in 0.5 N HCl without and with DTDBT inhibitor. The EDX examination manifests that the Fe element was the major element in the surface composition before and after the immersion in 0.5 M HCl solutions. Fig. 12A and B display the EDX spectrum with the chemical composition of the polished C-steel specimen without and with immersion in 0.50 M HCl. The elements existing in the surface of the C-steel sample before immersion in 0.5 M HCl were 0.046% P, 0.12% C, 1.27% Mn, and 98.56% Fe, Fig. 12A. The proportion of the elements has changed in the case of C-steel specimen immersed in 0.50 M HCl solution free or comprising 1×10^{-4} M DTDBT inhibitor. The presence of additional signals for O and Cl elements in Fig. 12B and C could be attributed to the oxidation of Fe on the steel surface by the effect of HCl solutions. On the other hand, the appearance of N and S signals

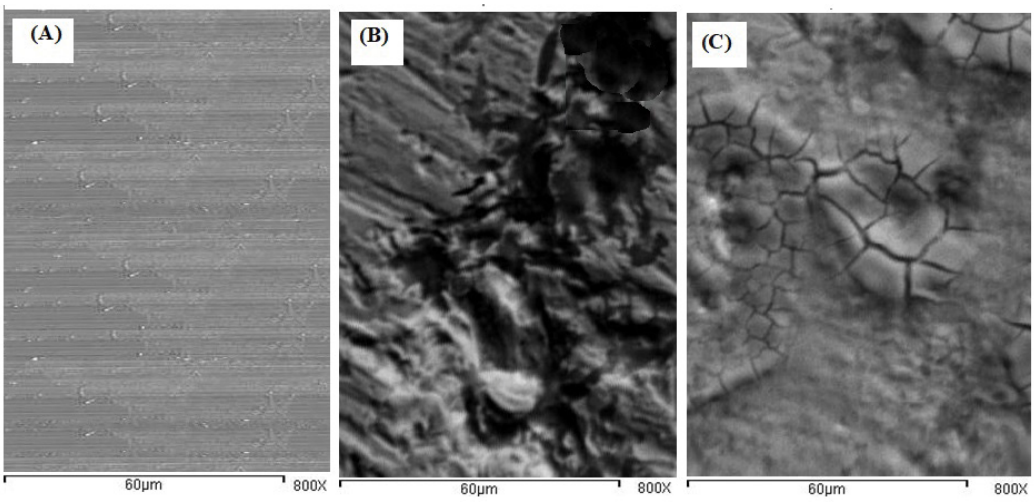

Fig. 11. SEM morphology of C-steel specimen before (A) and after inundation for 3 h in 0.5 M HCl solution devoid of (B) and containing 1×10^{-4} M DTDBT inhibitor (C), at 298 K.

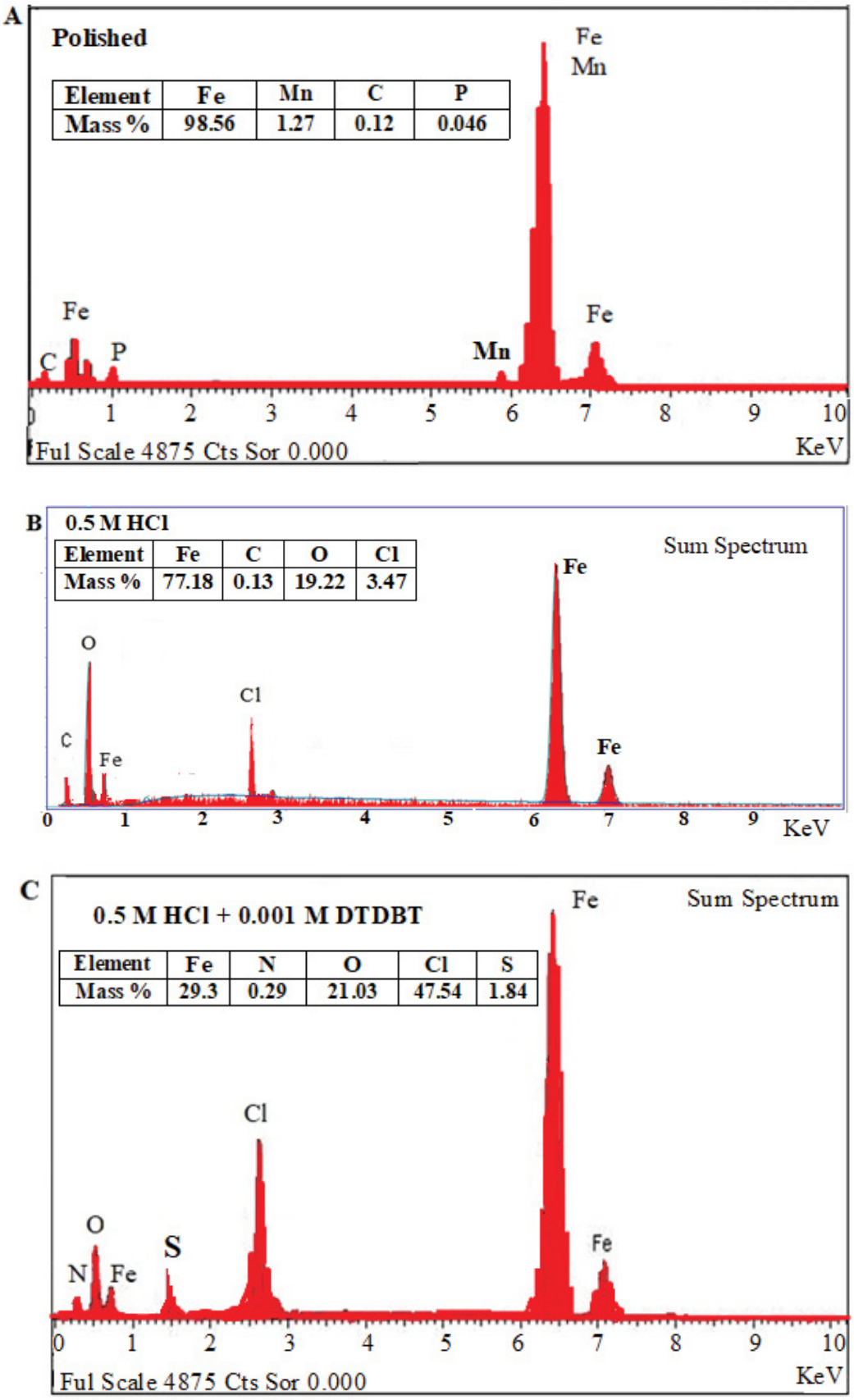

Fig. 12. (A) EDX spectra of C-steel before immersion in 0.5 M HCl solution. (B) EDX spectra of C-steel after immersion for 3 h in 0.5 M HCl. (C) EDX spectra of C-steel after immersion for 3 h in 0.5 M HCl containing 1×10^{-4} M DTDBT inhibitor, at 25°C.

after immersion of C-steel sample in 0.5 M HCl containing 1 × 10^{-4} M DTDBT inhibitor (Fig. 12C) confirms the existence of DTDBT inhibitor on the C-steel surface. However, the high reduction in the percentage of Fe element in the case of DTDBT inhibitor than that of the free acid sample, besides the appearance of the N and S signal could be related to the presence of a protective inhibitor film on the C-steel surface.

4. Conclusions

- The DTDBT inhibitor behaves as a mixed-kind inhibitor towards the destruction of C-steel in HCl solutions.
- The DTDBT molecules reduce each of the cathodic and anodic reactions.
- The inhibition efficacy of the DTDBT inhibitor is increased with the concentration but decreases with temperature.
- The adsorption of the DTDBT molecules obeyed Langmuir's model.
- The data of gravimetric, polarization and EIS methods were compatible.

Acknowledgments

The authors gratefully acknowledge the approval and support of this research study by the Grant No. (SCI-2018-3-9-F-7759) from the deanship of Science Research at Northern Border University, Arar, K.S.A.

Disclosure statement

No potential conflict of interest was reported by the author(s).

References

[1] M. Scendo, Inhibitive action of the purine and adenine for copper corrosion in sulphate solutions, Corros. Sci., 49 (2007) 2985–3000.
[2] A.A. Farag, M.A. Migahed, A.M. Al-Sabagh, Adsorption and inhibition behavior of a novel Schiff base on carbon steel corrosion in acid media, Egypt. J. Pet., 24 (2015) 307–315.
[3] M.A. Hegazy, A.M. Badawi, S.A. Abd El Rehim, W.M. Kamel, Corrosion inhibition of carbon steel using novel N-(2-(2-mercaptoacetoxy)ethyl)-N,N-dimethyl dodecan-1-aminium bromide during acid pickling, Corros. Sci., 69 (2013) 110–122.
[4] M. Finšgar, J. Jackson, Application of corrosion inhibitors for steels in acidic media for the oil and gas industry: a review, Corros. Sci., 86 (2014) 17–41.
[5] G. Schmitt, Application of inhibitors for acid media: report prepared for the European Federation of corrosion working party on inhibitors, Br. Corros. J., 19 (1984) 165–176.
[6] Kh. Rahmani, R. Jadidian, S. Haghtalab, Evaluation of inhibitors and biocides on the corrosion, scaling and biofouling control of carbon steel and copper–nickel alloys in a power plant cooling water system, Desalination, 3931 (2016) 174–185.
[7] S. Thirugnanaselvi, S. Kuttirani, A.R. Emelda, Effect of Schiff base as corrosion inhibitor on AZ31 magnesium alloy in hydrochloric acid solution, Trans. Nonferrous Met. Soc. China, 24 (2014) 1969–1979.
[8] M. Ajmal, A.S. Mideen, M.A. Quraishi, 2-Hydrazino-6-methylbenzothiazole as an effective inhibitor for the corrosion of mild steel in acidic solutions, Corros. Sci., 36 (1994) 79–84.
[9] Z. Hu, Meng, X. Ma, H. Zhu, J. Li, C. Li, D. CaO, Experimental and theoretical studies of benzothiazole derivatives as corrosion inhibitors for carbon steel in 1 M HCl, Corros. Sci., 112 (2016) 563–575.
[10] S. Abd El Wanees, A.A.H. Bukhari, N.S. Alatawi, S. Salem, S. Nooh, S.K. Mustafa, Thermodynamic and adsorption studies on the corrosion inhibition of Zn by 2,2′-dithiobis (2,3-dihydro-1,3-benzothiazole) in HCl solutions, Egypt. J. Chem., 64 (2021) 547–559
[11] B.V.A. Rao, M.Y. Iqbal, B. Sreedhar, Self-assembled monolayer of 2-(octadecyl-thio)benzothiazole for corrosion protection of copper, Corros. Sci., 51 (2009) 1441–1452.
[12] K.C. Emregul, O. Atakol, Corrosion inhibition of mild steel with Schiff base compounds in 1M HCl, Mater. Chem. Phys., 82 (2003) 188–193.
[13] R.S. Verma, H.M. Meshram, R. Dahiya, Solid state oxidation of thiols to disulfides using ammonium per-sulfate, Synth. Commun., 30 (2000) 1249–1255.
[14] S. Abd El Wanees, E.E. Abd El Aal, N-Phenylcinnamimide and some of its derivatives as inhibitors for corrosion of lead in HCl solutions, Corros. Sci., 52 (2010) 338–344.
[15] D.-Q. Zhang, Q.-R. Cai, X.-M. He, L.-X. Gao, G.S. Kim, Corrosion inhibition and adsorption behavior of methionine on copper in HCl and synergistic effect of zinc ions, Mater. Chem. Phys., 114 (2009) 612–617.
[16] S.M. Abd El Haleem, S. Abd El Wanees, E.E. Abd El Aal, A. Diab, Environmental factors affecting the corrosion behavior of reinforcing steel. IV. Variation in the pitting corrosion current in relation to the concentration of the aggressive and the inhibitive anions, Corros. Sci., 52 (2010) 1675–1683.
[17] L. Kord, M. Nasr-Esfahani, Corrosion behavior of carbon steel in HCl solution by Fe and Cr complexes with a Schiff-base ligand derived from salicylaldehyde and 2-(2-aminoethylamino) ethanol, Surf. Eng. Appl. Electrochem., 51 (2015) 491–500.
[18] S. Abd El Wanees, A. Diab, O. Azazy, M. Abd El Azim, Inhibition effect of N-(pyridin-2-yl-carbamothioyl) benzamide on the corrosion of C-steel in sulfuric acid solutions, J. Dispersion Sci. Technol., 35 (2014) 1571–1580.
[19] Y. Zhou, S. Zhang, L. Guo, S. Xu, H. Lu, F. Gao, Studies on the effect of a newly synthesized Schiff base compound on the corrosion of copper in 3% NaCl solution, Int. J. Electrochem. Sci., 10 (2015) 2072–2087.
[20] I. Ahamad, R. Prasad, M. Quraishi, Adsorption and inhibitive properties of some new Mannich bases of Isatin derivatives on corrosion of mild steel in acidic media, Corros. Sci., 52 (2010) 1472–1481.
[21] M. El Azhar, B. Mernari, M. Traisnel, F. Bentiss, M. Lagrenee, Corrosion inhibition of mild steel by the new class of inhibitors [2,5-bis(n-pyridyl)-1,3,4-thiadiazoles] in acidic media, Corros. Sci., 43 (2001) 2229–2238.
[22] S. Deng, X. Li, X. Xie, Hydroxymethyl urea and 1,3-bis(hydroxymethyl)urea as corrosion inhibitors for steel in HCl solution, Corros. Sci., 80 (2014) 276–289.
[23] M.A. Hegazy, M. Abdallah, M.K. Awad, M. Rezk, Three novel di-quaternary ammonium salts as corrosion inhibitors for API X65 steel pipeline in acidic solution. Part I: Experimental results, Corros. Sci., 81 (2014) 54–64.
[24] I. Ahamad, M.A. Quraishi, Bis(benzimidazol-2-yl) disulphide: an efficient water soluble inhibitor for corrosion of mild steel in acid media, Corros. Sci., 51 (2009) 2006–2013.
[25] N.M. EL Basiony, A. Elgendy, H. Nady, M.A. Migaheda, E.G. Zaki, Adsorption characteristics and inhibition effect of two Schiff base compounds on corrosion of mild steel in 0.5 M HCl solution: experimental, DFT studies, and Monte Carlo simulation, RSC Adv., 9 (2019) 10473–10485.
[26] P. Sakunthala, S.S. Vivekananthan, M. Gopiraman, N. Sulochana, A.R. Vincent, Spectroscopic investigations of physicochemical interactions on mild steel in an acidic medium by environmentally friendly green inhibitors, J. Surfactants Deterg., 16 (2013) 251–263.
[27] A.M. Guruprasad, H.P. Sachin, G.A. Swetha, B.M. Prasanna, Corrosion inhibition of zinc in 0.1 M hydrochloric acid medium with clotrimazole: experimental, theoretical and quantum studies, Surf. Interfaces, 9 (2020) 100478, doi: 10.1016/j.surfin.2020.100478.
[28] S. Abd El Wanees, N.M. El Basiony, A.M. Al-Sabagh, M.A. Alsharif, S.M. Abd El Haleem, M.A. Migahed, Controlling

of H_2 gas production during Zn dissolution in HCl solutions, J. Mol. Liq., 248 (2017) 943–952.
[29] E.E. Oguzie, Y. Li, F.H. Wang, Corrosion inhibition and adsorption behavior of methionine on mild steel, in sulfuric acid and synergistic effect of iodide ion, J. Colloid Interface Sci., 310 (2007) 90–98.
[30] E.E. Abd El Aal, S. Abd El Wanees, A. Farouk, S.M. Abd El Haleem, Factors affecting the corrosion behavior of aluminium in acid solutions. II. Inorganic additives as corrosion inhibitors for Al in HCl solutions, Corros. Sci., 68 (2013) 14–24.
[31] S.M. Abd El Haleem, S. Abd El Wanees, E.E. Abd El Aal, A. Farouk, *Factors affecting* the *corrosion behavior* of aluminium in acid solutions. I. Nitrogen and/or sulphur-containing organic compounds as *corrosion inhibitors* for *Al* in *HCl* solutions, *Corros.* Sci., 68 (2013) 1–13.
[32] A.K. Maayta, N.A.F. Al-Rawashdeh, Inhibition of acidic corrosion of pure aluminum by some organic compounds, Corros. Sci., 46 (2004) 1129–1140.
[33] J.O'M. Bockris, A.K.N. Reddy, M. Gamboa-Aldeco, Modern Electrochemistry, 2nd ed., Kluwer Academic/Plenum Publishers, New York, 2000.
[34] M.G. Saleh, S. Abd El Wanees, S.K. Mustafa, Dihydropyridine derivatives as controllers for production of hydrogen during zinc dissolution, Chem. Eng. Commun., 206 (2019) 789–803.
[35] L. Feng, S. Zhang, Y. Lu, B. Tan, S. Chen, L. Guo, Synergistic corrosion inhibition effect of thiazolyl-based ionic liquids between anions and cations for copper in HCl solution, Appl. Surf. Sci., 483 (2019) 901–911.
[36] E. Ech-chihbi, S. Nahlé, R. Salim, F. Benhiba, A. Moussaif, F. El-Hajjaji, H. Oudda, A. Guenbour, M. Taleb, I. Warad, A. Zarrouk, Computational, MD simulation, SEM/EDX and experimental studies for understanding adsorption of benzimidazole derivatives as corrosion inhibitors in 1.0 M HCl solution, J. Alloys Compd., 844 (2020) 155842, doi: 10.1016/j.jallcom.2020.155842.
[37] A.S. Fouda, M.A. Ismail, R.M. Abou-shahba, W.A. Husien, E.S. El-Habab, A.S. Abousalem, Experimental and computational chemical studies on the cationic furanylnicotinamidines as novel corrosion inhibitors in aqueous solutions, Chin. J. Chem. Eng., 28 (2020) 477–491.
[38] M. Faiz, A. Zahari, K. Awang, H. Hussin, Corrosion inhibition on mild steel in 1 M HCl solution by *Cryptocarya nigra* extracts and three of its constituents (alkaloids), RSC Adv., 10 (2020) 6547–6562.
[39] A. Ostovari, S.M. Hoseinieh, M.S. Peikari, R. Shadizadeh, S.J. Hashemi, Corrosion inhibition of mild steel in 1 M HCl solution by henna extract: a comparative study of the inhibition by henna and its constituents (lawsone, gallic acid, a-D-glucose and tannic acid), Corros. Sci., 51 (2009) 1935–1949.
[40] G. Moretti, F. Guidi, G. Grain, Tryptamine as a green iron corrosion inhibitor in 0.5 M deaerated sulphuric acid, Corros. Sci., 46 (2004) 387–403.
[41] A.S. Fouda, N. Nwar, M.A. Ismail, A.A. Zaher, A. Abousalem, The inhibition action of methoxy-substituted phenylthienyl benzamidines on the corrosion of carbon steel in hydrochloric acid medium, J. Mol. Liq., 312 (2020) 113267, doi: 10.1016/j.molliq.2020.113267.
[42] E.A. Noor, A.H. Al-Moubaraki, Thermodynamic study of metal corrosion and inhibitor adsorption processes in mild steel/1-methyl-4[4′(-X)-styryl pyridinium iodides/hydrochloric acid, Mater. Chem. Phys., 110 (2008) 145–154.
[43] L. Herrag, B. Hammouti, S. Elkadiri, A. Aouniti, C. Jama, H. Vezin, F. Bentiss, Adsorption properties and inhibition of mild steel corrosion in hydrochloric solution by some newly synthesized diamine derivatives: experimental and theoretical investigations, Corros. Sci., 52 (2010) 3042–3051.
[44] S.M.A. Hosseini, M. Salari, E. Jamalizadeh, S. Khezripoor, M. Seif, Inhibition of mild steel corrosion in sulfuric acid by some newly synthesized organic compounds, Mater. Chem. Phys., 119 (2010) 100–105.
[45] A. Addouna, S. Bouyegh, M. Dahmane, O. Ferroukhi, M. Trari, Thermodynamic investigation on the adhesion and corrosion inhibition properties of a non-steroidal anti-inflammatory drug in HCl electrolyte applied on mild steel material, Mater. Today Commun., 21 (2019) 100720, doi: 10.1016/j.mtcomm.2019.100720.
[46] G. Palumbo, K. Berent, E. Proniewicz, J. Bana´s, Guar gum as an eco-friendly corrosion inhibitor for pure aluminium in 1-M HCl solution, Materials, 12 (2019) 2620, doi: 10.3390/ma12162620.
[47] M.H.M. Hussein, M.F. El-Hady, M.A.H. Shehata, M.A. Hegazy, H.H.H. Hefni, Preparation of some eco-friendly corrosion inhibitors having antibacterial activity from sea food waste, Surf. Deterg., 16 (2013) 233–242.
[48] P. Shetty, Schiff bases: an overview of their corrosion inhibition activity in acid media against mild steel, Chem. Eng. Commun., 207 (2020) 985–1029.
[49] S Abd El Wanees, M.I. Alahmdi, S.M. Rashwan, M.M. Kamel, M.G. Abd Elsadek, Inhibitive effect of cetyltriphenylphosphonium bromide on C-steel corrosion in HCl solution, Int. J. Electrochem. Sci., 11 (2016) 9265–9281.
[50] S. Abd El Wanees, S.H. Seda, Corrosion inhibition of zinc in aqueous acidic media using a novel synthesized Schiff base–an experimental and theoretical study, J. Dispersion Sci. Technol., 40 (2019) 1813–1826.
[51] S.S. Abd El Rehim, S.M. Sayyah, M.M. El-Deeb, S.M. Kamal, R.E. Azooz, Adsorption and corrosion inhibitive properties of p(2-aminobenzothiazole) on mild steel in hydrochloric acid media, Int. J. Ind. Chem., 7 (2016) 39–52.